arXiv:1605.04990v4 [nlin.PS] 2 Mar 2017

# Bubble-like structures generated by activation of internal shape modes in two-dimensional sine-Gordon line solitons

Mónica A. García-Ñustes* and Juan F. Marín†
*Instituto de Física, Pontificia Universidad Católica de Valparaíso, Casilla 4059, Chile*

Jorge A. González‡
*Department of physics, Florida International University, Miami, Florida 33199, United States*

(Dated: March 3, 2017)

Nonlinear waves that collide with localized defects exhibit complex behavior. Apart from reflection, transmission, and annihilation of an incident wave, a local inhomogeneity can activate internal modes of solitons, producing many impressive phenomena. In this work, we investigate a two-dimensional sine-Gordon model perturbed by a family of localized forces. We observed the formation of bubble-like and drop-like structures due to local internal shape modes instabilities. We describe the formation of such structures on the basis of a one-dimensional theory of activation of internal modes of sG solitons. An interpretation of the observed phenomena, in the context of phase transitions theory, is given. Implications in Josephson junctions with a current dipole device are discussed.

PACS numbers: 05.45.Yv, 05.45.-a, 11.10.Lm

## I. INTRODUCTION

Nonlinear wave propagation in inhomogeneous media is of great importance in many branches of the natural sciences. Most physical systems are nonlinear and inhomogeneous. Therefore, realistic models usually require to introduce weak nonlinearities and inhomogeneities on its description [1].

The propagation of solitons has been widely investigated in the literature due to its important applications [2]. The study of the disturbances on traveling solitons by the presence of spatial inhomogeneities, like localized defects or boundary interphase walls, are of great interest in physics and biophysics [3–5]. Depending on the geometrical size and shape of such inhomogeneities, there can be annihilation or reflection of an incident nonlinear wave. These disturbances on the propagation regime may have important consequences for the behavior of the system [3, 5]. For instance, propagation of fluxons in Josephson junctions (JJ's) may be affected by spatial heterogeneities in the junction created by a current dipole device [6–8]. However, transmission, reflection, and annihilation are far from being the only possible phenomena that may occur when solitary waves collide with localized spatial inhomogeneities.

The particle-like behavior of solitons is a well-known property [2, 9]. Moreover, it has been proved that solitons behave more as extended objects rather than point-like particles. The activation of internal modes under the action of a family of topologically equivalent inhomogeneous forces was proved analytically for $\phi^4$ and sine-Gordon (sG) models [10, 11]. Such internal modes can lose stability, leading to very exciting phenomena as breaking of solitons, the creation of kink-antikink pairs and formation of multikinks as the two-kink soliton[12–14].

The sG model has been applied in many branches of physics as particle physics and condensed matter theory. The model can describe many phenomena in solid state physics as domain walls in ferromagnets and fluxons in long JJ's [6, 8, 15]. In high energy physics and cosmology, topological defects in Klein-Gordon (KG) systems are relevant in brane world scenarios and to describe phase transitions in the early universe [16–22].

In this work, we investigate the effect on the internal structure, and therefore on the dynamics, of a two-dimensional sG line solitons due to space-localized inhomogeneities. The study is based on an analytical model of solitons externally excited by a family of topologically equivalent forces in one dimension [11, 12]. We show that the soliton dynamics is highly enriched by the interplay between the activation of internal modes and the kink-antikink interactions. Shape modes instabilities lead to the formation of stable bubbles and drops. These are sustained by the presence of the inhomogeneity itself, being unstable otherwise. We also show that two-kink solutions[14, 23] can be also formed in two-dimensional systems, creating stable *two-kink bubbles*. The remainder of this paper is organized as follows. In section II we give a brief overview of the analytical theory of the activation of internal shape modes in one-dimensional sG solitons. We also introduce the two-dimensional model of the system and the numerical methods employed. In section III we show and discuss the results from numerical simulations. The robustness of the observed phenomena is discussed in section IV, and an interpretation of our results in the context of phase transitions is given. Finally, in section V we present our concluding remarks.

* monica.garcia@pucv.cl
† juanfmarinm@gmail.com
‡ jorgalbert3047@hotmail.com

## II. TWO-DIMENSIONAL MODEL AND THE ONE-DIMENSIONAL THEORY OF ACTIVATION OF SHAPE MODES

Consider the two-dimensional perturbed sG equation

$$\partial_{tt}\phi(\mathbf{r},t) = \nabla^2\phi(\mathbf{r},t) - \sin\phi(\mathbf{r},t) - \gamma\partial_t\phi(\mathbf{r},t) + F(\mathbf{r}), \quad (1)$$

where $\mathbf{r} = (x, y)$, $\gamma$ is a linear-damping coefficient and $F$ is an external space-dependent force. Line solitons, pulsons, ring solitons, and breathers are some examples of the many soliton solutions of equation (1) for $F(\mathbf{r}) = 0$ [24–26].

In one dimensional systems, when the inhomogeneous force is given by $F(x) = \pm 2(B^2-1)\sinh(Bx)\mathrm{sech}^2(Bx)$, the perturbed sG equation has the exact solutions $\phi_\pm(x) = 4\arctan\exp(\pm Bx)$ [11]. Here, $\phi_+$ and $\phi_-$ reads for the kink and antikink, respectively. $F(x)$ is an antisymmetric spatial function that vanishes exponentially for $x \to \pm\infty$ and has a single zero at $x_* = 0$. It is known that the zeros of the external force act as equilibrium positions for the soliton motion [10]. Thus, $x_*$ is an equilibrium position. In particular, if $F(x)$ possesses only one zero ($F(x_*) = 0$) and $\partial F(x)/\partial x\big|_{x=x_*} > 0$, then the point $x = x_*$ is a stable (unstable) equilibrium position for the kink (antikink). Otherwise, if $\partial F(x)/\partial x\big|_{x=x_*} < 0$, the equilibrium position $x = x_*$ is unstable (stable) for the kink (antikink). Thus, $B$ is a parameter that controls the extension of the force, its maximum amplitude, and the sign of its derivative at $x_*$.

For the following discussion we consider the case $\phi(x,0) = 4\arctan\exp(Bx)$ and $F(x) = 2(B^2-1)\sinh(Bx)\mathrm{sech}^2(Bx)$. For this force function, the stability analysis for kink internal modes can be solved exactly [11, 12]. For $B^2 > 1$, $F(x)$ has a positive slope around $x_*$, the translational mode is stable and there are no internal shape modes. In this regime, the soliton is trapped at the stable equilibrium position $x_*$. If $1/3 < B^2 < 1$, $F(x)$ has a negative slope around $x_*$. The translational mode of the kink is unstable. Still, no internal modes are present. The soliton moves from its equilibrium position without shape deformations. For $1/6 < B^2 < 1/3$, the first stable internal shape mode arises, while for $B^2 < 1/6$ many other internal modes can appear. For $B^2 < 2/[\Lambda_*(\Lambda_*+1)]$, where $\Lambda_* = (5+\sqrt{17})/2$, the first internal mode becomes unstable, leading to a soliton breakup and shape instabilities [10–12].

Following up the one-dimensional case, we will consider only line soliton solutions for the two-dimensional system, Eq.(1). To control the spreading of the inhomogeneous force in the y-direction we introduce a smooth decaying function. Consequently, the internal modes of the soliton will be activated locally, i.e., in a certain region of the kink front. Any rapidly decaying function can be used for this purpose, e.g. a Gaussian function, a superposition of Heaviside functions, or some spline polynomial. In our model, we have used a Gaussian function, since it is a physically realizable force. Therefore, the inhomogeneous force $F(x, y)$ is given by

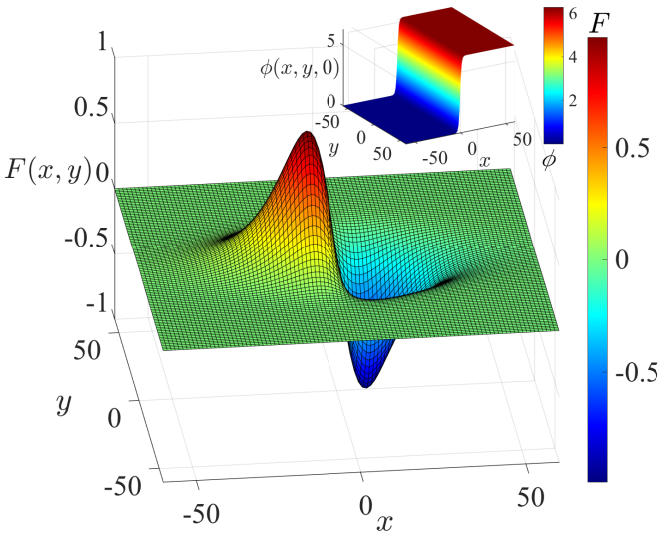


FIG. 1. (Color online) Inhomogeneous force of equation 2 for $B = 0.1$ and $\sigma = 15$. The inset show the static line soliton used as initial condition.

$$F(x,y) = \pm 2(B^2-1)\frac{\sinh(Bx)}{\cosh^2(Bx)}e^{-y^2/\sigma^2}, \quad (2)$$

where $B$ and $\sigma$ acts as control parameters. Given that $\sigma$ is a measure of the Gaussian width, it plays a controlling role of the local stability of the front. Force (2) is displayed in Figure 1. The perturbation of fluxons by dipole current devices in JJ's is a typical example of a strong and local external influence with the same topological form as expression (2) [8]. This forcing term may be also relevant for 1D models of biological molecules, like DNA chains, where 1D sG systems have been considered as a suitable model to explain the formation of open states or *bubbles* in the double helix [27–29]. Thus, results obtained in this work can be generalized to other topologically equivalent systems [11].

In the present paper, all numerical simulations are performed using a kink as the initial condition, and the perturbation $F(x,y) = 2(B^2-1)\sinh(Bx)\mathrm{sech}^2(Bx)e^{-y^2/\sigma^2}$. However, recall that the coefficient $2(B^2-1)$ becomes negative for $B^2 < 1$. This change will lead to the instabilities that we have discussed above. We have used finite differences of second order of accuracy to numerically solve equation (1) with no-flux boundary conditions. For the explicit difference schemes, we have used a regular mesh of size $l \times l$, with $l = 1200$. The space intervals are $\Delta x = \Delta y = 0.1$, and the time increment is $\Delta t = 0.02$. The initial conditions are given by $\phi(x,y,0) = 4\arctan\exp(x/L)$ and $\partial_t\phi(x,y,0) = 0$, where $L$ is an arbitrary parameter. This represents a stationary kink located at the equilibrium point $x_*$ (see inset Fig.1). Under these conditions, we avoid any scattering effect, focusing our attention on the dynamics of

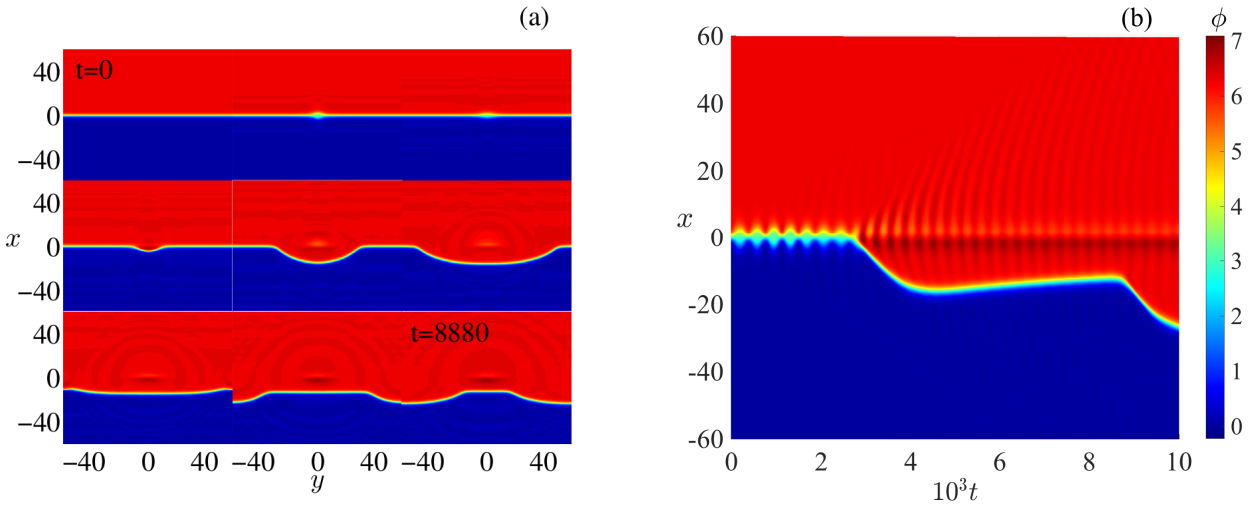


FIG. 2. (Color online) Locally unstable soliton ($B^2 = 0.5$ and $\sigma = 15$). (a) Snapshots from numerical simulations, taken each 1110 time iterations. (b) Time evolution of the $x$-profile of the soliton ($y = 0$). The value of the field $\phi$ is indicated in color scale.

the soliton internal structure. Notwithstanding, any stationary soliton located near the stable equilibrium point $x_*$ can be attracted and trapped by the inhomogeneity, setting up an initial condition as well. The damping term in equation (1) is introduced to dissipate the phononic excitations emitted by the mesh.

## III. NUMERICAL SIMULATIONS

In this section, we summarize the main results obtained from numerical simulations. As previously stated, $B$ and $\sigma$ act as control parameters. Thus, our parameter space is $\{B, \sigma\}$. It is expected that for a value of $\sigma$ large enough, we recover the one-dimensional results by varying $B$. For smaller values of $\sigma$, however, activation of internal modes will be only local.

### A. Stability of the translational mode

To check the numerical method, we started our simulations setting the following parameter values, $B = 1.2$ and $\sigma_{max} = 15$. This value reproduces an extended enough force in comparison with the mesh size $l$ and it represents our $\sigma$ upper limit. According to the one-dimensional theory, for $B^2 > 1$, it is expected that the translational mode to be stable, whereas no shape internal modes are present. Indeed, the line soliton translational mode is stable for $B = 1.2$. No front motion is observed.

Next, we decrease the value of $B$. According to the 1D theory, for $1/3 < B^2 < 1$ the translational mode is locally unstable.

Two-dimensional numerical simulations show that for $1/3 < B^2 < 1$, the localized force *always* destabilizes the translational mode of the soliton, despite the value of $\sigma$. This is a surprising result since one would expect that a sufficiently localized perturbation could not destabilize an extended object. The lattice coupling would prevent the kink front motion if the perturbation is sufficiently local. However, this is not the case.

In figure 2 we show the results obtained for $B^2 = 0.5$ and $\sigma = 15$. The soliton translational mode is locally unstable around the origin, as expected from the one-dimensional theory. Since the force is localized in space, the kink front turns unstable locally. In figure 2(a) we see that this local instability travels in the $y$-direction with a certain velocity, destabilizing the whole kink front progressively. The perturbation eventually reflects on the boundaries, and travels backward. In figure 2(b), we display the $x$-profile for $y = 0$. We can observe that the line soliton core experiences a small oscillation before the whole front begins to move. Such oscillation, which amplitude is decaying in time, is produced by an interaction between the local destabilization and the lattice. Eventually, the local instability overcomes the lattice coupling coefficient and the front starts to move after around 2000 time iterations. Figure 2(b) also reveals a curvature effect, exhibited by the small return of the front to the origin. Such effect will be described more extensively in the subsequent section. The last bursting is produced by the reflection of the perturbation in the walls.

### B. Bubble and drop formation

For $1/6 < B^2 < 1/3$, the stable first internal shape mode arises, which becomes unstable for $B^2 < 2/[\Lambda_*(\Lambda_* + 1)]$, where $\Lambda_* = (5 + \sqrt{17})/2$. Consequently, for $0 < \sigma \leq \sigma_{max}$, the line soliton will exhibit more com-

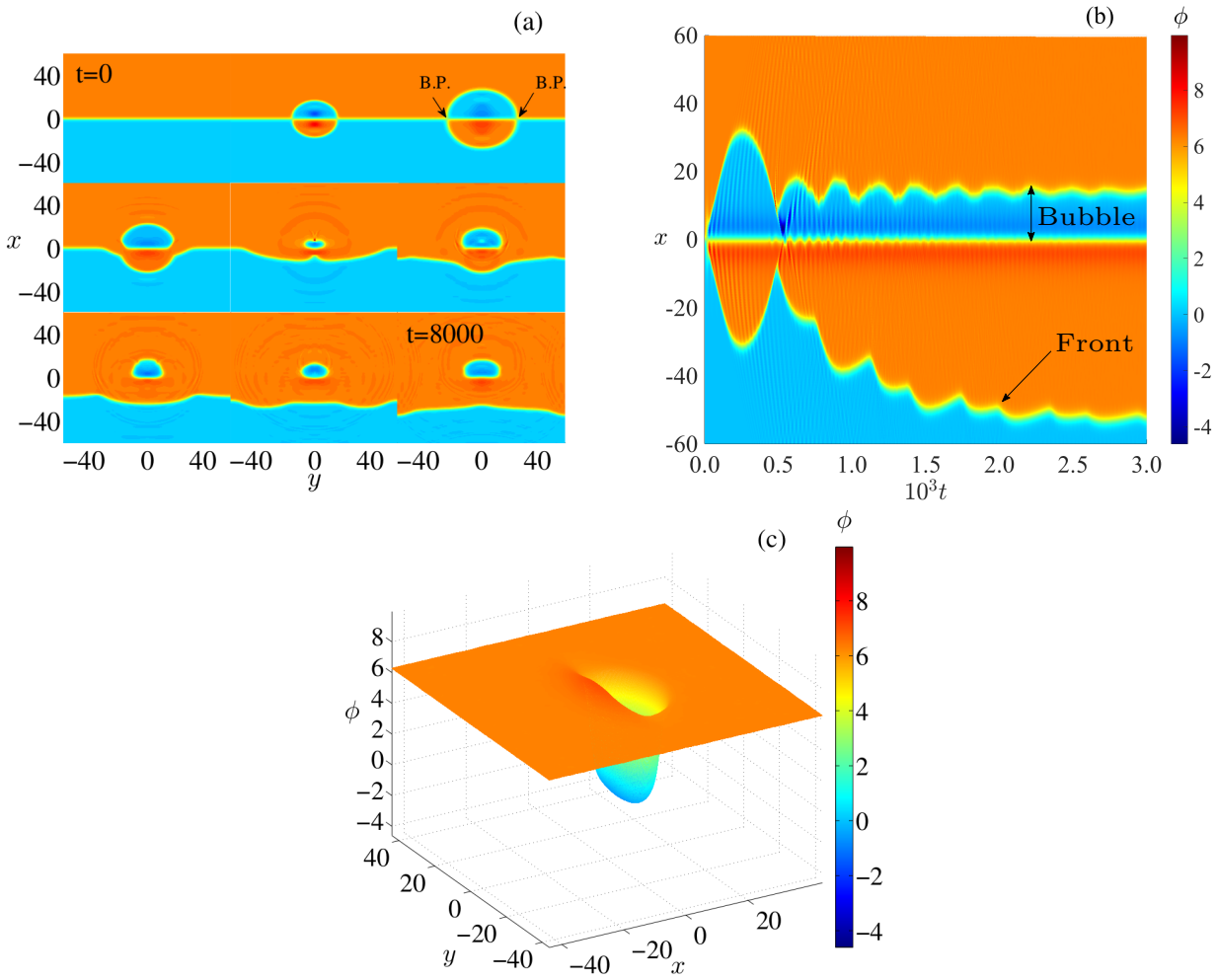


FIG. 3. (Color online) Bubble formation for $B = 0.27$ and $\sigma = 15$. (a) Snapshots from numerical simulations, taken each 1000 time iterations. (b) Time evolution of the $x$-profile of the soliton for $y = 0$. (c) Bubble-like structure after 30000 time iterations. The value of the field $\phi$ is indicated in color scale.

plex phenomena due to the local destabilization of an internal shape mode. Effectively, the local instability of the shape mode leads to a local break-up of the front. This initial breaking travels through the lattice, developing finally a stable *bubble-like structure*. In figure 3(a), we can observe the formation of a stable bubble-like structure for $B = 0.27$ and $\sigma = 15$. Initially, we observe the formation of an elliptic-like structure that grows around the inhomogeneity. The initial small oscillation is not present because the instability is strong enough to overcome rapidly the lattice coupling coefficient. In this scenario, the curvature of the structure plays an important role in the dynamics. The radial velocity decreases such that a maximum size of the elliptic structure is reached, and then the structure collapses backward. This effect is known in the literature as the *return-effect* [30], and is produced entirely by the curvature of the elliptic front. During this collapse, the elliptic structure separates from the front in two breaking points (BP) showed in figure 3(a).

Formation and time-evolution of the bubble-like structure can also be seen in figure 3(b). We show the $x$-profile of the soliton at $y = 0$ as a function of time. We can see that around the first 5000 time iterations, the elliptical-type form grows and collapses, following by the formation of the bubble. The bubble-like structure is formed in the positive region of $x$ and its size is initially oscillating due to reminiscent perturbations produced during its formation. These oscillations decrease in time, and the structure remains stable with a fixed size and shape (fig. 3(c)). The oscillating process is depicted in Fig.4.

To evaluate the role of parameter $\sigma$ and $B$ over the formation of bubble-like structures, we proceed to vary both parameters separately. Figure 4 shows the temporal evolution of the major $R_y$ and minor $R_x$ semi-axis of the elliptical structure. We observe that the bubble formation process is the same in all cases but not the bubble final size. In Fig. 4(a) we have varied parameter

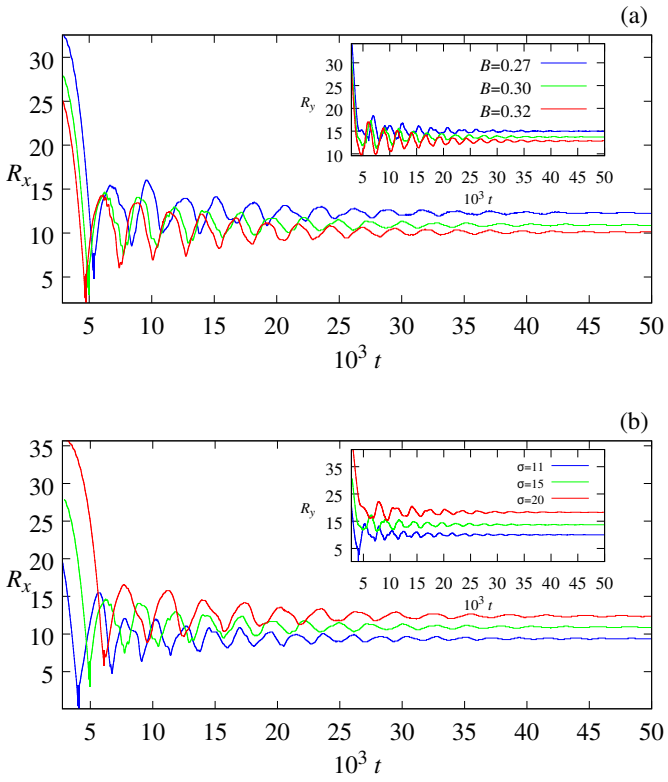


FIG. 4. (Color online) Evolution of the semi-axis of bubbles as a function of time for different values of parameters $B$ and $\sigma$. (a) Evolution of $R_x$ and $R_y$ (inset) for $\sigma = 15$. (b) Evolution of $R_x$ and $R_y$ (inset) for $B = 0.27$.

$B$ leaving $\sigma = 15$ fixed. We can observe that both $R_x$ and $R_y$ oscillate on time. However, after this initial transient state, the system evolves to a determined size. It is clear that as we increase $B$, $R_x$ and $R_y$ decrease, reducing the final bubble area. On the contrary, when we vary $\sigma$, leaving $B$ fixed, the opposite occurs. Figure 4(b) shows the temporal evolution of $R_x$ and $R_y$ of the bubble structure for $B = 0.27$ fixed. As $\sigma$ gets smaller, we can see that the final bubble area also decreases.

However, if we continue diminishing $\sigma$, leaving $B$ in the range where the first internal mode is unstable, the preferred structure is one with the reverse polarity–in terms of the topological charge–a *drop-like structure*. Figure 5(a) shows the formation of a stable drop-like structure for $B = 0.28$ and $\sigma = 8.9$. As we can observe, the mechanism of drop formation is similar to that of the bubble-like structure. After the collapse of the elliptical form, a stable drop-like structure is formed in the negative region of $x$, in contrast with the bubble formation (see Fig. 5(b)). From inset in Fig. 5(b) is clear that the drop-like formation is produced after the total collapse of the initial bubble, suggesting a kink-antikink collision between the bubble walls. Subsequently, the kink-antikink merge with the same velocity but a phase shift, enhancing a drop-like structure. In Fig. 5(c), we depicted the final stage of the drop-like structure.

From this result, we can infer that the final bubble area, and therefore $\sigma$ and $B$, are playing an important role in determining which kind of structure will be formed, either bubble or drop-like. This will be further discussed in section III D.

### C. Bubble-drop bound states

Until now we have observed the formation of isolated drops or bubbles in a certain range of the parameter space $\{B, \sigma\}$. Still, further diminishing the value of $B$, with fixed $\sigma$, we have found a coexistence region where a bubble and a drop merge in a stable structure–*a bubble-drop bound state*. In figure 6(a) we display the bubble-drop bound state formation for $B = 0.2$ and $\sigma = 10$. From the one-dimensional theory, it is known that below $B = 0.2564$, the formation of two-kink solitons occurs. As expected, the typical elliptic-like structure grows to exhibit a two-kink profile. One two-kink connects the states $2\pi$ and 0, and also the states 0 and $-2\pi$, as it can be seen in figure 6(b). Meanwhile, an additional two-kink connects the states $4\pi$ and 0, passing through $2\pi$. However, after a transient, this last state breaks, the $0 - 2\pi$ kink moves along the negative x-direction while the $2\pi - 4\pi$ kink forms a drop. Conversely, both kinks in the positive x-direction remain oscillating around their positions until reach a stable state–*a two-kink bubble*. Finally, we get a two-kink bubble and a single drop forming a stable bound state (see Fig.6(c)). We have observed also multi-structures, like a *multi-kink bubble*, for smaller values of $B$.

### D. Discussion

We can understand the formation of bubbles and drops by considering the following mechanism. The initial condition used in our simulations is a $2\pi$-kink connecting two stable states in phase space, namely $\phi_0 = 0$ and $\phi_1 = 2\pi$. Since the inhomogeneous force is localized around the origin, the internal modes of the soliton become unstable only in a neighborhood of the origin. The instability of the internal shape mode leads to a kink-antikink pair formation. The local antikink remains steady in the origin and it will constitute part of the bubble. This kink zone will propagate until the localized forced is weak enough to the return effect and kink-interaction come to play. At this stage, the ellipse walls start to move backward. If $\sigma$ is large enough or $B$ small, the walls will reach a steady position, forming a stable bubble. The final area of this bubble will depend on both parameters, $\sigma$ and $B$. Under a critical value of the elliptical area, the kink-antikink interaction is strong enough to produce the bubble collapse. As we have mentioned before, this enables the formation of a drop-like structure due to a phase shift during the

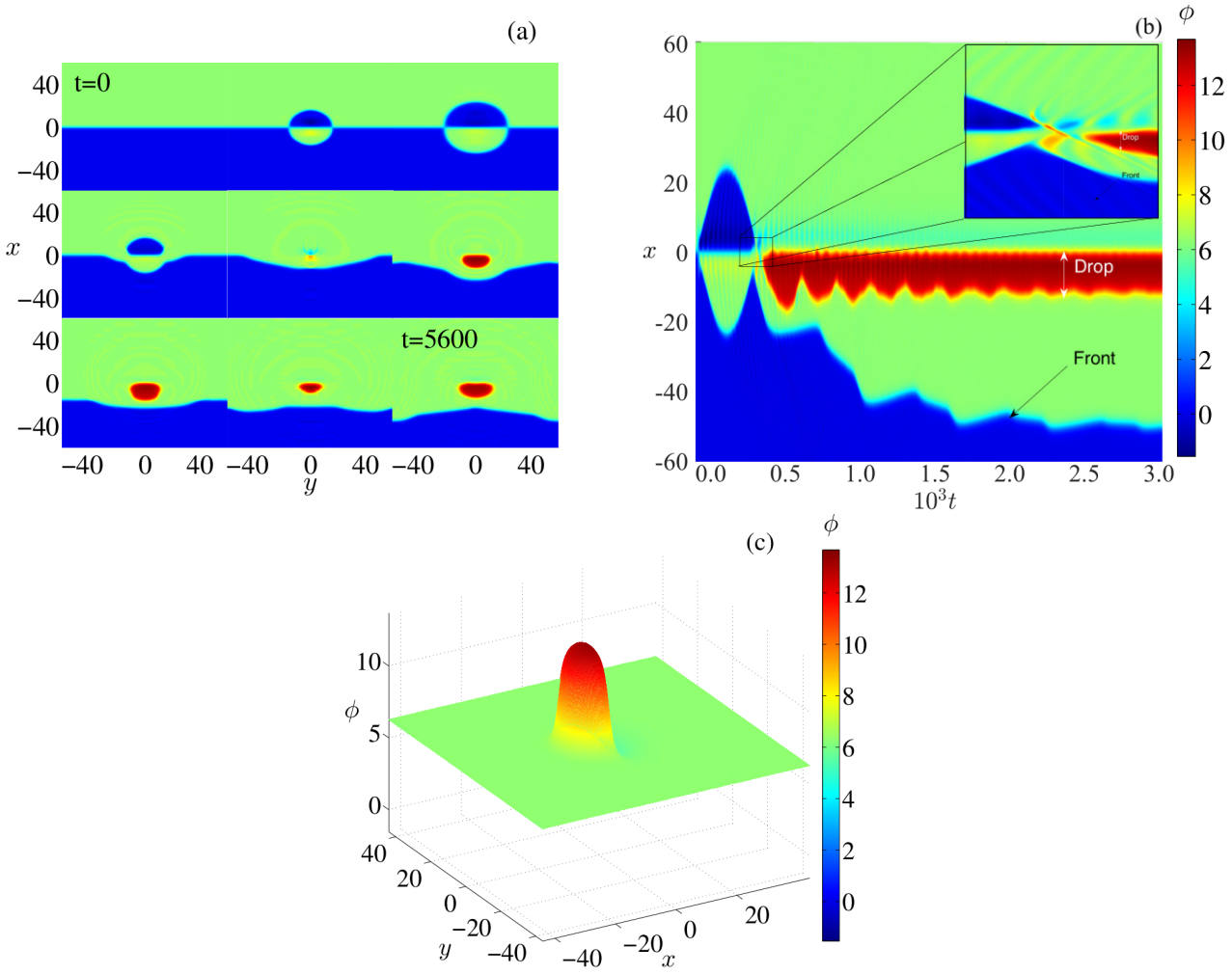


FIG. 5. (Color online) Drop formation ($B = 0.28$ and $\sigma = 8.9$). (a) Snapshots from numerical simulations, taken each 700 time iterations. (b) Time evolution of the $x$-profile of the soliton for $y = 0$. Inset: Zoom of the kink-antikink collision during bubble collapse. (c) Drop-like structure after 30000 time iterations. The value of the field $\phi$ is indicated in color scale.

kink-antikink collision. Therefore, the value of parameters $B$ and $\sigma$ will determine which kind of structure will be formed.

The external force $F(x, y)$ sustains the bubble and it acts as an opposite force of the kink-antikink interaction. The interplay between both forces: one pulling inwards–kink-antinkink interaction–and the other pulling outwards–external force–create a stable equilibrium-the bubble state. In fact, $F(x, y)$ is predominant in the bubble final shape. Based on this, we can infer that $R_x$ is controlled by the force (2) for $y = 0$. Thus, the semi-minor axis $R_x$ will be proportional to the decaying coefficient of $F_0(x) \equiv F(x, 0)$, $d_x = 1/B$, therefore $R_x \sim 1/B$. Meanwhile, $R_y$ is controlled by the Gaussian function. The maximum of $F(x, y)$ is located at $x_M = 2.94$. This represents the point where the Gaussian function has its maximum extension. The decaying coefficient of $F_M(y) \equiv F(2.94, y)$ is $d_y = 1/\sqrt{1/\sigma^2} = \sigma$. Thus, $R_y \sim \sigma$. As we can see, $F_M(y)$ possesses a slower decaying tail than $F_0(x)$, hence, the elliptical form of the bubble. Figures 4(a) and 4(b), respectively, corroborate these statements.

We also notice that the shrinking force due to return effect, along with the external inhomogeneous force, produce an oscillation of the two-kink pairs in the two-bubble structures. However, they finally stabilize forming *two-kink bubbles* (see figure 7).

We performed numerical simulations for several combinations of values of $B$ and $\sigma$ and obtained the qualitative parameter space map showed in figure 8. All different kind of structures has been depicted. We notice that for large $\sigma$, the results are in good agreement with the predictions of the one-dimensional theory. This is an expected result since the system behaves as a quasi-one-dimensional system in this region of parameter space. We notice in figure 8 that there are no stable structures below a certain value of $\sigma$. We have calculated this minimum value $\sigma_c$ by considering the kink-antikink interaction en-

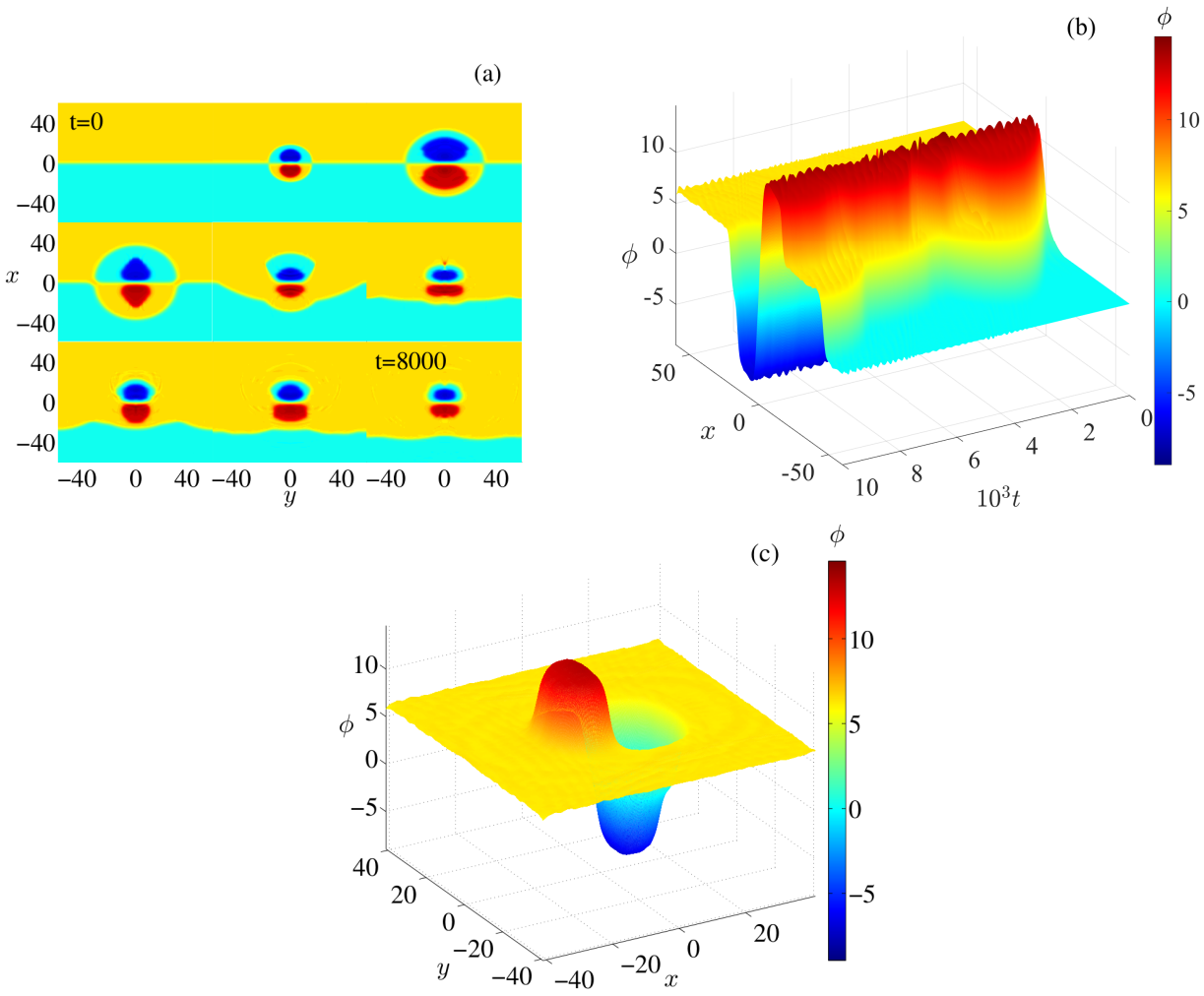


FIG. 6. (Color online) Pair bubble-drop formation ($B = 0.2$ and $\sigma = 10$). (a) Snapshots from numerical simulations, taken each 1000 time iterations. (b) Time evolution of the $x$-profile of the soliton ($y = 0$). The formation of multikinks is clearly seen. (c) Pair bubble-drop structure after 30000 time iterations. The value of the field $\phi$ is indicated in color scale.

ergy, $E_{int}(a) = -16(\sinh(a) + a)\sinh^{-1}(a)(\cosh(a) + 1)^{-1}$, where $a$ is the distance between cores [31]. The kink-antikink interaction tends to collapse the bubbles, while $F_0(x)$ tends to sustain them. Thus, we expect that stable structures can be formed when one equilibrates the other. Indeed, the function $F_0(x)$ intersect $F_{int} = dE_{int}/da$ only in a certain interval $[\sigma_c, \infty)$. By a careful analysis of the intersection interval, we obtained that $\sigma_c \simeq 3.7$, which is in agreement with the results depicted in figure 8. Under this minimum value, any structure will eventually collapse, since the inhomogeneity $F$ never equilibrates the kink-antikink attractive force.

## IV. FORMATION OF BUBBLES AND DROPS IN RELATED SYSTEMS

It is noteworthy that the formation of bubbles and drops in our system is a robust phenomenon. Results similar to the ones presented in this article can be obtained in other systems using other external perturbations with the same topological properties of force (2). In the following, we briefly discuss some theoretical studies that corroborate these findings.

### A. Robust phenomena in dynamical systems

The sG equation (1) is a particular case of the more general nonlinear KG equation

$$\partial_{tt}\phi(\mathbf{r},t) - \nabla^2\phi(\mathbf{r},t) + \gamma\partial_t\phi(\mathbf{r},t) - G(\phi) = F(\mathbf{r}), \quad (3)$$

where $G(\phi) = -\partial U(\phi)/\partial\phi$, and the nonlinear potential $U(\phi)$ possesses at least two minima separated by a barrier. These two minima are fixed points of the associated dynamical system, and it is well known that kink solutions are heteroclinic trajectories joining such fixed

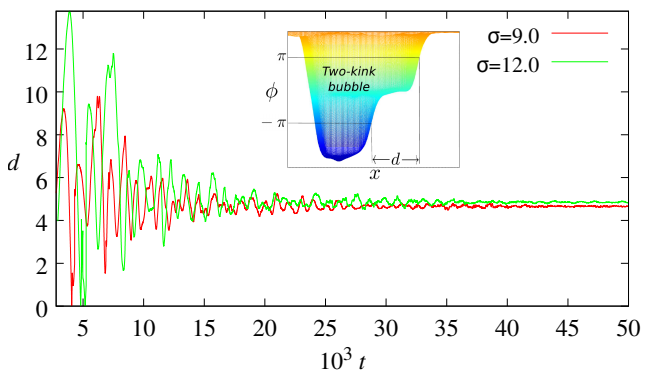


FIG. 7. (Color online) Separation of kinks in a two-kink bubble as a function of time for $B = 0.24$. The distance $d$ between the cores of the kinks (inset) evolve in time before reaching a constant value. Although the final separation is a small value compared to the total size of the system, the structure is clearly stable.

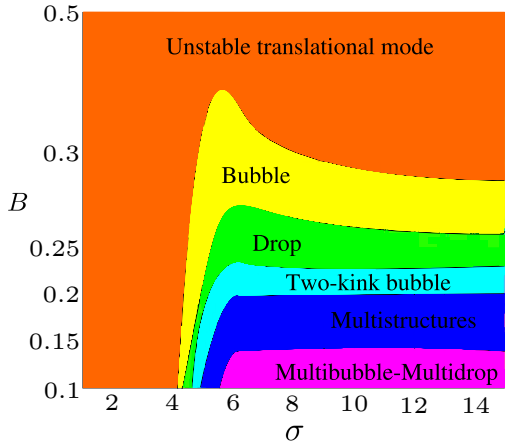


FIG. 8. (Color online) Qualitative view of the parameter space map, obtained on the basis of numerical simulations. Six main zones are observed, each one corresponding to different kind of structures. Bubbles and drops become more complex as increasing $\sigma$ and decreasing $B$.

points [32]. Therefore, a complete investigation of equations of type (3) can be performed using the so-called qualitative theory of dynamical systems [33]. Knowing the behavior of kink solutions in the neighborhood of fixed points and separatrices, it is possible to construct other functions with the same general properties of the exact solutions of equation (3). Thus, it is possible to generalize the results to other equations that are topologically equivalent to those with the exact solutions [34]. Therefore, we conclude that the same structure formation reported in this article can be observed qualitatively using more general forces expressed as follows:

$$F(x,y) = f(x)g(y), \tag{4}$$

where $g(y)$ is an exponentially decaying function such that $\lim_{y\to\pm\infty} g(y) = 0$. Thus, the general topological properties of $f(x)$ are the following: (a) $f(x)$ should have a zero accompanied by a local minimum and a local maximum. (b) Must be localized, i.e. $\lim_{x\to\pm\infty} f(x) = 0$. Note that the function given by equation (2) is a particular case of this class of functions. The relevant parameters are the slope of the function at the equilibrium point $x = x_*$ and the values of the maximum and the minimum.

To give a particular example of the above discussion, let us briefly consider in the force (4) the functions

$$f(x) = A\left[-\frac{1}{\cosh^p[b(x+d)]} + \frac{1}{\cosh^p[b(x-d)]}\right], \tag{5}$$

$$g(y) = \operatorname{sech}\left(\frac{y}{s}\right). \tag{6}$$

Notice that with these functional profiles, force (4) fulfills all required properties. Parameters $A$ and $d$ control the value of the local maximum of $F(x,y)$ and its $x$-coordinate position, respectively. The spread of the force in the $x$ direction is controlled by parameters $b$ and $p$, while in the $y$-direction is controlled by $s$. In figure 9 we reproduce qualitatively the same results discussed in this work for the reported values of parameters.

Giving that the discussed phenomena can occur for more general forces, we conclude that $f(x)$ does not have to be exactly $F(x) = 2(B^2-1)\sinh(Bx)\operatorname{sech}^2(Bx)$. For example, the $F(x,y)$ discussed in this work is a very good approximate model of the current dipole device created by Ustinov and collaborators [7, 8], which can be implemented in JJ's experiments. The technique of insertion of fluxons into annular JJ's proposed in [7] can be theoretically understood as the creation of a fluxon-antifluxon pair due to internal modes instabilities. The development of methods that allow for the construction of exact solutions to the equation (3) for a general $F(\mathbf{r})$ and the investigation of the topological influence of the actual shape of the experimental forcing is an open problem that requires more research work in the future.

### B. Sine-Gordon solitons in phase transitions

Equation (3) also appears in the description of structural phase transitions, where a central question is whether the system can be driven to a new phase by some instability [13, 35].

In the vicinity of a first order phase transition, a metastable state of matter can be obtained by means of nonlinear excitations. The main phenomenon is that of *nucleation*, where bubbles and drops can grow or disappear. A *critical germ* is commonly considered for the development of a given instability that is energetically above a *nucleation barrier*, in order to produce a transition from one phase to another. If the field configuration $\phi(\mathbf{r},t)$ has a radius larger than the critical germ, the instability will grow and a phase transition will occur [36].

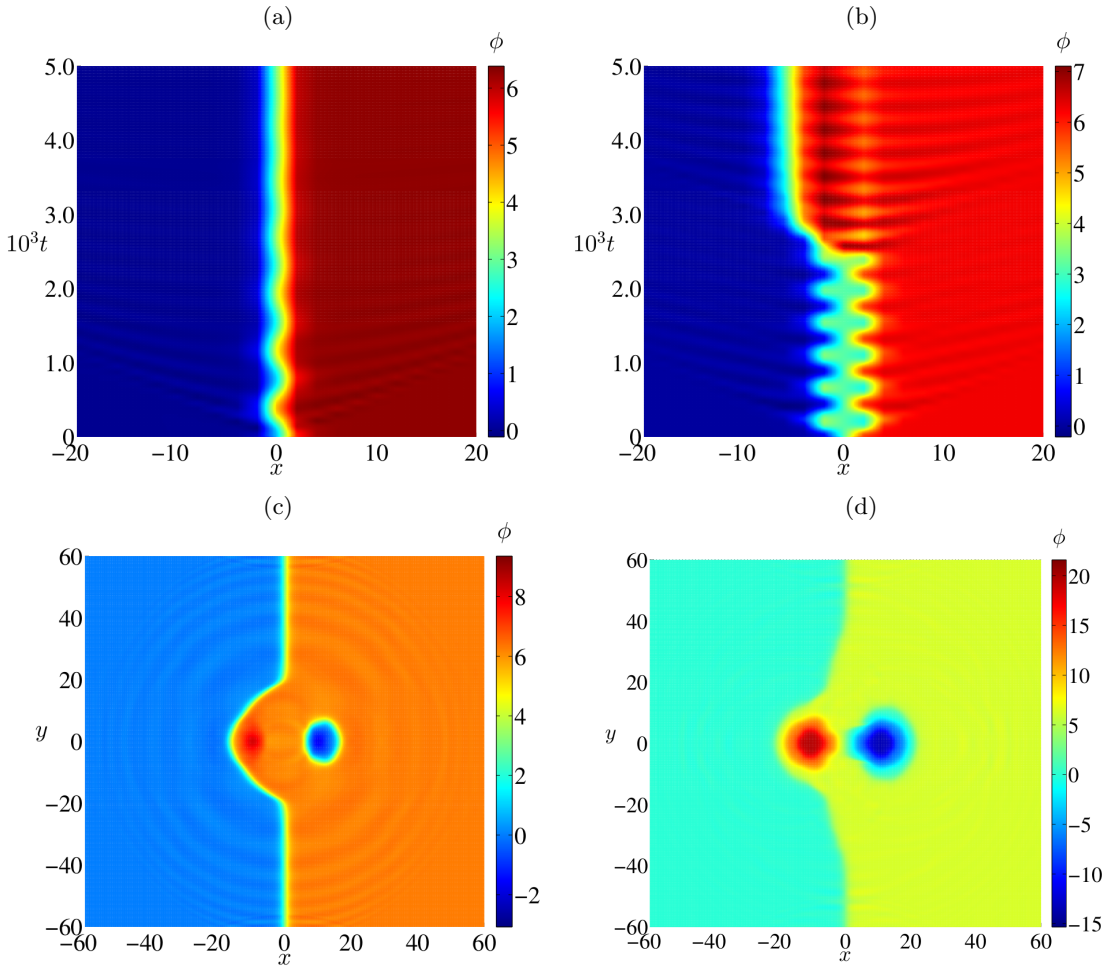


FIG. 9. (Color online) Kink-dynamics and formation of localized structures in a topologically equivalent sG system (equations (1), (4), (5) and (6)). (a) Time evolution of the $x$-profile of an initially-at-rest kink placed at $x_o = 0.6$ for $A = 1.05$, $b = 1$, $d = 0.5$, $p = 2$ and $s = 10$. The point $x_* = 0$ is a stable fixed point for the kink. The soliton performs damping oscillations around $x_*$. (b) Time evolution of the $x$-profile of a locally unstable kink for $A = -0.9$, $b = 0.1$, $d = 2.0$, $p = 200$ and $s = 0.5$. A change of stability occurs due to the change of sign in the derivative of the force at $x_*$, and the fixed point is now unstable (see equivalent phenomenon in figure 2). (c) A bubble-like structure at $t = 4000$ for $A = -1.2$, $b = s = 0.28$, $p = 2$ and $d = 10$ (see equivalent phenomenon in figure 3). (d) A multistructure (bound state) at $t = 4000$ for $A = -1.5$, $b = s = 0.28$, $p = 2$ and $d = 10$ (see equivalent phenomenon in figure 6).

In the case of the sG system (1), the potential is given by $U(\phi) = 1 - \cos\phi$ [2], and we have several barriers, i. e., unstable states, that separate stable states. Unstable stationary solutions that connect any two of these stable states are, indeed, kink-antikink pairs with a drop-like or bubble-like structure. These solutions play the role of a critical germ for the transition from one state to the other [10, 35, 37]. Unstable regions in parameter space can be interpreted as intervals for parameters $\sigma$ and $B$ where the force produces drops and bubbles with a smaller size than the critical germ, so they collapse. In the case where these structures are larger than the critical germ, the attractive force between kinks and antikinks are balanced by the external force, so the structure is sustained by the inhomogeneity. This property has been used in real experiments of controlled transport of bubbles using laser beams in weak absorbing liquids [13], where a first-order liquid-vapour phase transitions are induced. We expect that a time-dependent force with a spatial profile similar to equation (2) would be useful to transport the bubble-like and drop-like structures reported in this work.

## V. CONCLUSIONS AND FINAL REMARKS

By means of numerical simulations, we have shown that the internal structure of two-dimensional sine-Gordon solitons affects the dynamics of the wave when interacting with localized inhomogeneities. We have observed the formation of bubble and drop-like structures that are sustained by the force, being unstable otherwise. The formation of these structures are entirely due to in-

ternal mode instabilities of the solitary wave, and it has no relation with any scattering effect. We have given a qualitative explanation of the formation of such structures using an analytical model of the breaking of solitons by topologically equivalent inhomogeneities. From our simulations, we have demonstrated that the two-kink solutions can be also stable in two-dimensional systems. For the observed phenomena, we have given an interpretation in the context of the phase transitions theory. We expect to observe the formation of bubbles and drops in related solitonic systems, like the $\phi^4$ model. Of course, the existence of multi-structures will depend on the existence of many stable states in phase space. Thus, we do not expect to find a two-kink bubble structure in a two-dimensional $\phi^4$ model, as well as it is not expected to find multikinks in the one-dimensional model [14].

As a final remark, the phenomena observed in this work may have important implications in two-dimensional JJ's devices. The formation of bubbles in the junction due to a dipole current and the trapping and breaking of such structures by such localized inhomogeneities may produce important effects on the functioning of the device. Moreover, the study of the stability and transport of such bubbles can shed light on the design of built-in heterogeneities and control of perturbations in the junction. Fluxon transmission in JJ's devices can also be regulated by the application of this kind of external perturbations.

## ACKNOWLEDGMENTS

The authors thank Irving Rondón for fruitful discussions. M.A.G-N. thanks for the financial support of FONDECYT project 11130450. J.F.M. acknowledge financial support of CONICYT doctorado nacional 21150292.

[1] G. Nicolis, *Introduction to nonlinear science* (Cambridge University Press, 1995).
[2] M. Peyrard and T. Dauxois, *Physique des Solitons* (Savoirs actuels, 2004).
[3] V. Ivancevic and T. Ivancevic, J. Geom. Symmetry Phys. **31**, 1 (2013).
[4] O. V. Aslanidi and O. A. Mornev, J. Biol. Phys. **25**, 149 (1999).
[5] O. A. Mornev, L. M. Tsyganov, O. Aslanidi, A. E. Ordanovich, and L. M. Chailakhyan, Dokl. Biophys. **373**, 32 (2000).
[6] A. Barone and G. Paternò, *Physics and applications of the Josephson effect* (Wiley, 1982).
[7] A. V. Ustinov, Appl. Phys. Lett. **80**, 3153 (2002).
[8] B. A. Malomed and A. V. Ustinov, Phys. Rev. B **69**, 064502 (2004).
[9] M. Remoissenet, *Waves called solitons: concepts and experiments* (Springer Science & Business Media, 2013).
[10] J. A. González and J. A. Holyst, Phys. Rev. B **45**, 10338 (1992).
[11] J. A. González, A. Bellorín, and L. E. Guerrero, Phys. Rev. E **65**, 065601 (2002).
[12] J. A. González, A. Bellorín, and L. E. Guerrero, Chaos Soliton Fract. , 907 (2003).
[13] J. González, A. Marcano, B. Mello, and L. Trujillo, Chaos Soliton Fract. **28**, 804 (2006).
[14] M. A. García-Ñustes and J. A. González, Phys. Rev. E **86**, 066602 (2012).
[15] J. A. González, M. A. García-Ñustes, A. Sánchez, and P. V. E. McClintock, New J. Phys. **10**, 113015 (2008).
[16] T. Kibble, Phys. Rep. **67**, 183 (1980).
[17] V. A. Gani and A. E. Kudryavtsev, Phys. Rev. E **60**, 3305 (1999).
[18] V. A. Gani, A. E. Kudryavtsev, and M. A. Lizunova, Phys. Rev. D **89**, 125009 (2014).
[19] V. A. Gani, V. Lensky, and M. A. Lizunova, J. High Energy Phys. **147** (2015), 10.1007/JHEP08(2015)147.
[20] G. P. de Brito, R. A. C. Correa, and A. de Souza Dutra, Phys. Rev. D **89**, 065039 (2014).
[21] G. de Brito and A. de Souza Dutra, Phys. Lett. B **736**, 438 (2014).
[22] S. U. Galiev, *Darwin, Geodynamics and Extreme Waves* (Springer International Publishing, 2015).
[23] D. Bazeia, J. Menezes, and R. Menezes, Phys. Rev. Lett. **91**, 241601 (2003).
[24] P. L. Christiansen and P. S. Lomdahl, Physica D **2**, 482 (1981).
[25] N. Martinov and N. Vitanov, J. Phys. A Math. Gen. **25**, L419 (1992).
[26] J. M. Tamga, M. Remoissenet, and J. Pouget, Phys. Rev. Lett. **75**, 357 (1995).
[27] R. V. Polozov and L. V. Yakushevich, J. Theor. Biol. **130**, 423 (1988).
[28] L. V. Yakushevich, *Nonlinear Physics of DNA* (Wiley–VCH, 2004).
[29] A. A. Grinevich, A. A. Ryasik, and L. V. Yakushevich, Chaos Soliton Fract. **75**, 62 (2015).
[30] P. Christiansen and O. Olsen, Phys. Lett. A **68**, 185 (1978).
[31] M. Bordag and J. M. Muñoz Castañeda, J. Phys. A Math. Theor. **45**, 374012 (2012).
[32] W. van Saarloos and P. C. Hohenberg, Phys. Rev. Lett. **64**, 749 (1990).
[33] J. Guckenheimer and P. Holmes, *Nonlinear Oscillations, Dynamical Systems, and Bifurcations of Vector Fields* (Springer-Verlag New York, 1986).
[34] J. González, A. Bellorín, and L. Guerrero, Chaos Solitons Frac **33**, 143 (2007).
[35] J. A. González and F. A. Oliveira, Phys. Rev. B **59**, 6100 (1999).
[36] A. E. Filippov, Y. E. Kuzovlev, and T. K. Soboleva, Phys. Lett. A **165**, 159 (1992).
[37] J. A. González and J. Estrada-Sarlabous, Phys. Lett. A **140**, 189 (1989).